Unimolecular Chemistry of Protonated Glycine and Its Neutralized Form in the Gas Phase

Šárka Beranová, Jinnan Cai, and Chrys Wesdemiotis*

Contribution from the Department of Chemistry, The University of Akron, Akron, Ohio 44325-3601

Received February 9, 1995[⊗]

Abstract: Protonated glycine is produced in the gas phase by fast atom bombardment or chemical ionization (with CH_5^+), and its structures and unimolecular reactions are investigated by a combination of tandem mass spectrometry methods, including metastable ion (MI) characteristics, collisionally activated dissociation (CAD), and neutralization-reionization mass spectrometry (NRMS). The major fragmentations of $[H_2NCH_2COOH]H^+$ are elimination of CO to form the ion−molecule complex $H_2O\cdots{}^+H_2N{=}CH_2$ and consecutive cleavages of $H_2O + CO$ to yield the immonium ion $^+H_2N{=}CH_2$. Other important reactions involve the losses of $H^\bullet$, $H^\bullet + H_2O$, $H_2N^\bullet$, $H_2N^\bullet + H_2O$, $^\bullet COOH$, and CH_5N. Due to the facile H^+ migration possible in $[H_2NCH_2COOH]H^+$, the precise site of protonation cannot unequivocally be pinpointed based on the unimolecular reactions of this ion. More definitive information is obtained from the chemistry of neutralized $[H_2NCH_2COOH]H^+$. Analysis of this neutral by NRMS reveals that it consists of $^\bullet H_3NCH_2COOH$ and $H_2NCH_2C^\bullet(OH)_2$ at the moment of neutralization. Thus, the original protonation process must have created both tautomers. Once formed, the hypervalent ammonium radical $^\bullet H_3NCH_2COOH$ (neutral counterpart of N-protonated glycine) dissociates completely to $H^\bullet + H_2NCH_2COOH$ and H_3NCH_2 (or H_2NCH_3) + $^\bullet COOH$. On the other hand, the dihydroxy alkyl radical $H_2NCH_2C^\bullet(OH)_2$ (neutral counterpart of O-protonated glycine) undergoes several distinctive fragmentations, e.g., to $H_2N^\bullet + C_2H_4O_2$ and $H_2NCH_2^\bullet + CO + H_2O$.

Introduction

Elucidation of peptide and protein sequences from the dissociation patterns of protonated peptide ions is a particularly useful and wide-spread application of mass spectrometry.[1,2] The dissociation behavior of a protonated peptide is controlled by the nature of its constituent amino acids. For this reason, knowledge of the gas phase reactivities of protonated amino acids is of fundamental interest. So far, numerous experimental and theoretical studies have investigated the proton affinities and possible site(s) of protonation of amino acids;[3−14] however, information on the precise unimolecular reactions of H^+ cationized amino acids remains scarce. This article presents the first detailed examination of the gas phase chemistry of protonated glycine, the simplest amino acid.

Protonated glycine, $[H_2NCH_2COOH]H^+$ ($\mathbf{1}^+$), has been produced in the gas phase by a variety of ionization methods, including chemical ionization (CI),[15−18] secondary ion mass spectrometry (SIMS),[19] laser desorption (LD),[20] fast atom bombardment (FAB),[21] and plasma desorption (PD).[22] In these studies ion $\mathbf{1}^+$ was mainly used to probe the characteristics of the particular technique and its suitability for the mass spectral analysis of biologically important compounds.

The gas phase unimolecular reactions of cation $\mathbf{1}^+$ have been discussed only briefly in conjunction with other amino acids.[15−17,20−22] In contrast, the proton affinity (PA) of glycine, and of the other common α-amino acids, has been the principal subject of several studies for over a decade.[3−14] Proton-transfer equilibria between glycine and appropriate reference bases have confined PA(Gly) within 861−887 kJ mol^{-1},[3−5,8,12,13] relative to $PA(NH_3)$ = 853.5 kJ mol^{-1}.[5] This range is in accord with proton affinity orders[6,7,13] established from unimolecular dissociation rates of proton-bound heterodimers containing Gly and another amino acid (kinetic method[23]).

Either of glycine's two functional groups can bind the added proton. N-protonation generates the ammonium ion $\mathbf{1a}^+$ and O-protonation the resonance-stabilized dihydroxycarbenium ion $\mathbf{1b}^+$.[24] By comparing the proton affinity of H_2NCH_2COOH to the PAs of methylamine (896 kJ mol^{-1}) and acetic acid (796 kJ mol^{-1}),[5] Locke and McIver suggested that the site of

[⊗] Abstract published in *Advance ACS Abstracts*, September 1, 1995.

(1) Biemann, K. *Meth. Enzymol.* **1990**, *193*, 351−360, 455−479.
(2) Desiderio, D. M., Ed. *Mass Spectrometry of Peptides*; CRC Press: Boca Raton, 1991.
(3) Meot-Ner, M.; Hunter, E. P.; Field, F. H. *J. Am. Chem. Soc.* **1979**, *101*, 686−689.
(4) Locke, M. J.; McIver, R. T. *J. Am. Chem. Soc.* **1983**, *105*, 4226−4232.
(5) Lias, S. G.; Liebman, J. F.; Levin, R. D. *J. Phys. Chem. Ref. Data* **1984**, *13*, 695−808.
(6) Bojesen, G. *J. Am. Chem. Soc.* **1987**, *109*, 5557−5558.
(7) Isa, K.; Omote, T.; Amaya, M. *Org. Mass Spectrom.* **1990**, *25*, 620−628.
(8) Gorman, G. S.; Speir, J. P.; Turner, C. A.; Amster, I. J. *J. Am. Chem. Soc.* **1992**, *114*, 3986−3988.
(9) Campbell, S.; Beauchamp, J. L.; Rempe, M.; Lichtenberger, D. L. *Int. J. Mass Spectrom. Ion Processes* **1992**, *117*, 83−99.
(10) Bouchonnet, S.; Hoppilliard, Y. *Org. Mass Spectrom.* **1992**, *27*, 71−76.
(11) Jensen, F. *J. Am. Chem. Soc.* **1992**, *114*, 9533−9537.
(12) Wu, J.; Lebrilla, C. B. *J. Am. Chem. Soc.* **1993**, *115*, 3270−3275.
(13) Zhang, K.; Zimmerman, D. M.; Chung-Phillips, A.; Cassady, C. J. *J. Am. Chem. Soc.* **1993**, *115*, 10812−10822.
(14) Somogyi, A.; Wysocki, V. H.; Mayer, I. *J. Am. Soc. Mass Spectrom.* **1994**, *5*, 705−717.
(15) Milne, G. W. A.; Axenrod, T.; Fales, H. M. *J. Am. Chem. Soc.* **1970**, *92*, 5170−5175.
(16) Leclerq, P. A.; Desiderio, D. M. *Org. Mass Spectrom.* **1973**, *7*, 515−533.
(17) Tsang, C. W.; Harrison, A. G. *J. Am. Chem. Soc.* **1976**, *98*, 1301−1308.
(18) Vairamani, M.; Srinivas, R.; Viswanadha Rao, G. K. *Indian J. Chem.* **1988**, *27B*, 264−265.
(19) Benninghoven, A.; Sichtermann, W. K. *Anal. Chem.* **1978**, *50*, 1180−1184.
(20) Parker, C. D.; Hercules, D. M. *Anal. Chem.* **1985**, *57*, 698−704.
(21) Kulik, W.; Heerma, W. *Biomed. Environ. Mass Spectrom.* **1988**, *15*, 419−427.
(22) Bouchonnet, S.; Denhez, J.-P.; Hoppilliard, Y.; Mauriac, C. *Anal. Chem.* **1992**, *64*, 743−754.
(23) McLuckey, S. A.; Cameron, D.; Cooks, R. G. *J. Am. Chem. Soc.* **1981**, *103*, 1313−1317.

0002-7863/95/1517-9492$09.00/0

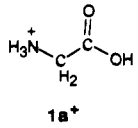

1a$^+$

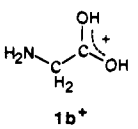

1b$^+$

protonation in the gas phase should be the amino and not the carbonyl substituent.[4] This assumption was supported by later studies of Beauchamp et al.,[9] who found a linear correlation between the proton affinities and the adiabatic lone pair ionization energies for amino acids protonating on the amine group. Further substantiation came from theory which predicts that the ammonium ion **1a**$^+$ is 58−75 kJ mol^{-1} more stable than the carbenium ion **1b**$^+$.[10,11,13,14] Whether **1a**$^+$ is exclusively formed upon ionization has, however, not been answered yet. Early CI studies by Tsang and Harrison[17] documented extensive intramolecular hydrogen exchange prior to fragmentation; this in turn was interpreted as indicative of the involvement of more than one structure for **1**$^+$, at least for short-lived ions.[17] By investigating the detailed unimolecular chemistry of [Gly]H$^+$, the present study attempts to also shed more light onto the structure(s) of ion **1**$^+$ produced upon FAB and CH_4-CI ionization as well as the structures traversed during unimolecular decomposition.

The gas phase structure(s) and reactions of FAB and CI generated **1**$^+$ and variously deuterated isotopomers are interrogated by three tandem mass spectrometry (MS/MS) methods,[25] namely metastable ion (MI) characteristics,[26] collisionally activated dissociation (CAD),[25] and neutralization−reionization mass spectrometry (NRMS).[27−29] MI and CAD assess the *ionic fragments* arising upon the spontaneous (in MI) or collisionally induced (in CAD) fragmentation of [Gly]H$^+$. The NRMS method allows (i) the identification of the *neutral fragments* coproduced upon dissociation of **1**$^+$ as well as (ii) the determination of the stability and reactivity of the *neutralized form* of **1**$^+$. The neutral losses are made detectable by collision-induced dissociative ionization (CIDI).[30] Pioneered by Holmes and Terlouw, CIDI has so far provided key insight on the structures and decomposition mechanisms of organic[30−32] as well as larger biomolecular[33,34] and polymeric[35] precursor ions. On the other hand, the neutral counterpart of the precursor ion is elucidated by neutralization−reionization (NR).[27−29] This neutral intermediate often yields fragments which are not formed from the precursor ion itself, thereby generating additional structural information that cannot be obtained from MI or CAD spectra alone.[36−39]

Experimental Section

The experiments were performed with a modified VG AutoSpec tandem mass spectrometer that has been described in detail.[40] This trisector E_1BE_2 instrument houses three collision cells, one (Cls-1) in the field-free region preceding E_1 (FFR-1) and two (Cls-2 and Cls-3), separated by an intermediate deflector electrode, between the magnet and E_2 (FFR-3). MS/MS measurements (MI, CAD, NRMS) are performed in FFR-3, by utilizing the first two sectors as MS-1 and the second electric sector as MS-2. MS/MS/MS studies are also possible by forming the precursor ion in FFR-1 and assessing its dissociations in FFR-3.

The [Gly]H$^+$ ion was produced by CI using methane as the reagent gas or by FAB with a Cs^+ ion gun operated at 20 kV. For FAB generated [H_2NCH_2COOH]H$^+$ (**1**$^+$), a few milligrams of glycine powder were dissolved in ~1 mL of glycerol and acidified with a droplet of aqueous HCl to enhance protonation; 1−2 μL of the resulting solution were then applied onto the probe tip and introduced into the ion source. Deuterated isotopomers were prepared by FAB in an analogous fashion: [D_2NCD_2COOD]D$^+$ (**4**$^+$) was obtained from glycine-d_5 with glycerol-d_3 and DCl, while mixed isotopomers [H_2NCD_2COOH]H$^+$ (**2**$^+$) and [D_2NCH_2COOD]D$^+$ (**3**$^+$) were generated by *in situ* H/D exchange, from glycine-d_5 + glycerol + HCl and glycine + glycerol-d_3 + DCl, respectively.

For NRMS spectra, 8 keV precursor ions were selected by MS-1 and subjected to collisions in Cls-2. With helium targets, these collisions mainly effect decomposition,[41] giving rise to ionic and neutral fragments. After removal of the ionic fragments and any residual precursor ions by electrostatic deflection, the remaining neutral fragments were post-ionized by CIDI with O_2 in Cls-3. The newly formed cations were mass-analyzed by MS-2 and recorded in the neutral fragment-reionization (N_fR He/O_2) mass spectrum of the precursor ion under study.[33−35] Such a spectrum contains the convoluted CIDI spectra[30,42] of the individual neutral losses liberated upon dissociation of the precursor ion. Neutralization−reionization (NR) mass spectra were obtained similarly by replacing He with trimethylamine (TMA), which exhibits high charge exchange cross sections.[43] Normal MI and CAD spectra were acquired employing no collision gas or O_2 in Cls-3, respectively. Kinetic energy releases were calculated from peak widths at half-height ($T_{0.5}$) and, for dish-topped signals, also across the dish maxima (T_{dish}); the values given for Gaussian signals were corrected for the main beam width using established procedures.[26b,c]

In MS/MS/MS experiments, the fragment ion of interest was formed by spontaneous dissociation or CAD with He in FFR-1 and then transmitted to FFR-3, where it underwent dissociating collisions in Cls-3. In CAD and NRMS measurements, the pressure of each target gas was adjusted to 20% attenuation of the main beam; this corresponds to nearly single collision conditions.[26c] All spectra were acquired with the slits completely open for maximum sensitivity; under these conditions, the main beam width at half height is 14 V. The spectra

(24) According to the studies of De Koster et al., direct protonation of a carboxylic acid (e.g., by CI) generates solely the C=O protonated form. Therefore, HO-protonated glycine, $H_2NCH_2C(=O)OH_2^+$, is not considered. See: De Koster, C. G.; Terlouw, J. K.; Levsen, K.; Halim, H.; Schwarz, H. *Int. J. Mass Spectrom. Ion Processes* **1984**, *61*, 87−95 and references therein.

(25) Busch, K. L.; Glish, G. L.; McLuckey, S. A. *Mass Spectrometry/Mass Spectrometry*; VCH Publishers: New York, 1988.

(26) (a) Cooks, R. G.; Beynon, J. H.; Caprioli, R. M.; Lester, G. R. *Metastable Ions*; Elsevier: Amsterdam, 1973. (b) Holmes, J. L.; Terlouw, J. K. *Org. Mass Spectrom.* **1980**, *15*, 383−396. (c) Holmes, J. L. *Org. Mass Spectrom.* **1985**, *20*, 169−183.

(27) Wesdemiotis, C.; McLafferty, F. W. *Chem. Rev.* **1987**, *87*, 485−500.

(28) Terlouw, J. K.; Schwarz, H. *Angew. Chem., Int. Ed. Engl.* **1987**, *26*, 805−815.

(29) Holmes, J. L. *Mass Spectrom. Rev.* **1989**, *8*, 513−539.

(30) Burgers, P. C.; Holmes, J. L.; Mommers, A. A.; Terlouw, J. K. *Chem. Phys. Lett.* **1983**, *102*, 1−3.

(31) (a) Burgers, P. C.; Holmes, J. L.; Hop, C. E. C. A.; Terlouw, J. K. *Org. Mass Spectrom.* **1986**, *21*, 549−555. (b) Wesdemiotis, C.; Feng, R.; Danis, P. O.; Williams, E. R.; McLafferty, F. W. *Org. Mass Spectrom.* **1986**, *21*, 689−695. (c) Holmes, J. L.; Hop, C. E. C. A.; Terlouw, J. K. *Org. Mass Spectrom.* **1986**, *21*, 776−778.

(32) Van Baar, B. L. M.; Terlouw, J. K.; Akkök, S.; Zummack, W.; Schwarz, H. *Int. J. Mass Spectrom. Ion Processes* **1987**, *81*, 217−225.

(33) Cordero, M. M.; Houser, J. J.; Wesdemiotis, C. *Anal. Chem.* **1993**, *65*, 1594−1601.

(34) Cordero, M. M.; Wesdemiotis, C. *Anal. Chem.* **1994**, *66*, 861−866.

(35) Selby, T. L.; Wesdemiotis, C.; Lattimer, R. P. *J. Am. Soc. Mass Spectrom.* **1994**, *5*, 1093−1101.

(36) Wesdemiotis, C.; Danis, P. O.; Feng, R.; Tso, J.; McLafferty, F. W. *J. Am. Chem. Soc.* **1985**, *107*, 8059−8066.

(37) Hop, C. E. C. A.; Holmes, J. L.; Terlouw, J. K. *J. Am. Chem. Soc.* **1989**, *111*, 441−445.

(38) Zhang, M.-Y.; Wesdemiotis, C.; Marchetti, M.; Danis, P. O.; Ray, J. C., Jr.; Carpenter, B. K.; McLafferty, F. W. *J. Am. Chem. Soc.* **1989**, *111*, 8341−8346.

(39) Hop, C. E. C. A.; Chen, H.; Ruttink, P. J. A.; Holmes, J. L. *Org. Mass Spectrom.* **1991**, *26*, 679−687.

(40) Polce, M. J.; Cordero, M. M.; Wesdemiotis, C.; Bott, P. A. *Int. J. Mass Spectrom. Ion Processes* **1992**, *113*, 35−38.

(41) (a) Danis, P. O.; Feng, R.; McLafferty, F. W. *Anal. Chem.* **1986**, *58*, 348−354. (b) Hop, C. E. C. A.; Holmes, J. L. *Org. Mass Spectrom.* **1991**, *26*, 476−480.

(42) Burgers, P. C.; Holmes, J. L.; Mommers, A. A.; Szulejko, J. E.; Terlouw, J. K. *Org. Mass Spectrom.* **1984**, *19*, 442−447.

(43) Wong, T.; Terlouw, J. K.; Weiske, T.; Schwarz, H. *Int. J. Mass Spectrom. Ion Processes* **1992**, *113*, R23-.

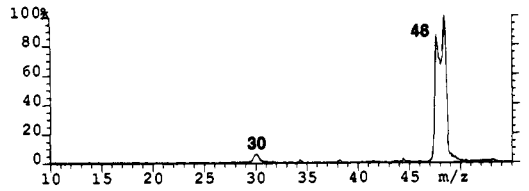

Figure 1. MI spectrum of $[H_2NCH_2COOH]H^+$, 1^+, formed by FAB. Very similar relative abundances are observed for CH_4-CI generated 1^+. Dissociation takes place in FFR-3.

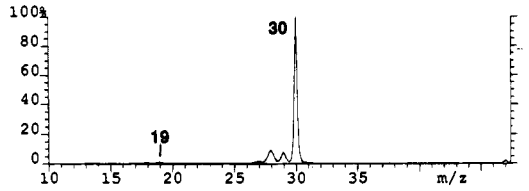

Figure 2. CAD spectrum (in FFR-3) of the $[1^+-CO]^+$ cation formed from metastable 1^+ in FFR-1. The same MS/MS/MS spectrum is obtained for $[1^+-CO]^+$ generated from collisionally activated 1^+.

shown are multiscan summations and their relative abundances are reproducible within ±15%.

Results and Discussion

A recommended approach for the elucidation of gas phase ion chemistry problems encompasses the use of several tandem mass spectrometry techniques in conjunction with isotopic labeling.[26c] In the present study the following four variously labeled isotopomers were investigated in order to probe the unimolecular chemistry of protonated glycine.

$[H_2NCH_2COOH]H^+$ $[H_2NCD_2COOH]H^+$
1^+ 2^+
$[D_2NCH_2COOD]D^+$ $[D_2NCD_2COOD]D^+$
3^+ 4^+

Reactions of Metastable Ions. The major spontaneous decomposition of FAB and CI generated 1^+ involves elimination of CO to produce CH_6NO^+ at *m/z* 48 (Figure 1). This reaction gives rise to a wide, dish-topped signal, with T_{dish} and $T_{0.5}$ equal to 176 and 459 meV, respectively. The $T_{0.5}$ value is in very good agreement with the 458 meV found previously for metastable 1^+ formed by FAB.[21] In order to establish the structure of the fragment ion arising upon CO loss, the CH_6NO^+ product was prepared in FFR-1 and examined by CAD in FFR-3. The resulting MS/MS/MS spectrum (Figure 2) is identical within experimental error to the published CAD spectrum[44] of the ion/dipole complex $H_2O\cdots{}^+H_2N{=}CH_2$, indicating that CO loss from 1^+ is accompanied by substantial molecular reorganization. Indeed, the peak shape and large kinetic energy release observed for this reaction agree well with a tight rearrangement associated with a large reverse activation energy.[26] Further, the cleavage of CO is more compatible with the N-protonated isomer $\mathbf{1a}^+$ which possesses an intact carbonyl group. All these facts are reconciled by the mechanism shown in Scheme 1. Note that the release of CO involves H-transfer and is not a least-motion extrusion, which would have produced $^+H_3N{-}CH_2{-}OH$; a similar behavior has been reported for the decarbonylation of ionized acetamide.[46]

Scheme 1[a]

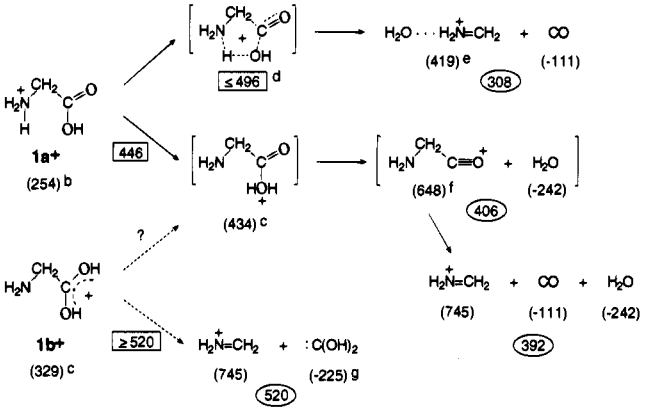

[a] The numbers in parentheses are heats of formation. $\sum\Delta H_f°$ values and transition state energies are shown in ovals and rectangles, respectively. All energies are in kJ mol^{-1} and from ref 45, unless otherwise noted. [b] Calculated from the experimentally determined PA of Gly (885 kJ mol^{-1}), assuming that this value corresponds to the N-protonated isomer $\mathbf{1a}^+$. [c] Obtained by adding to $\Delta H_f°(\mathbf{1a}^+)$ the theoretically predicted energy difference between $\mathbf{1a}^+$ and carbonyl protonated Gly ($\mathbf{1b}^+$) or hydroxyl protonated Gly, respectively.[10] [d] 446 + 50 (see text). [e] Reference 44. [f] Estimated from $\Delta H_f°(C_2H_5CO^+)$ = 591 kJ mol^{-1},[45] by assuming that the heats of formation of $H_2NCH_2CO^+$ and $C_2H_5CO^+$ differ by the same value as do the heats of formation of H_2NCH_2COOH and C_2H_5COOH. [g] Reference 48a.

A second, minor fragment in the MI spectrum of 1^+ corresponds to the immonium ion $^+H_2N{=}CH_2$, appearing at *m/z* 30 as a Gaussian signal (Figure 1).[47] The simplest route to this fragment would be a one-step fragmentation from O-protonated glycine, viz $\mathbf{1b}^+ \rightarrow {}^+H_2N{=}CH_2 + :C(OH)_2$. Such a reaction would liberate dihydroxycarbene, which was recently shown to be a stable molecule.[48] The very low dissociation yield of metastable 1^+ prevented us from identifying this neutral loss by a NRMS type experiment. It is worth mentioning, however, that collisionally activated 1^+, which produces ~10^3 times more $^+H_2N{=}CH_2$, contains no appreciable amount of complete CH_2O_2 molecules ($:C(OH)_2$ or HCOOH) in its neutral loss mixture (*vide infra*).

A detailed theoretical study by Bouchoux et al.[49] has examined the mechanism by which CH_2O_2 is cleaved from protonated leucine and isoleucine upon formation of their immonium ions. It was found that the elimination of intact $:C(OH)_2$ or HCOOH proceeds over a much higher barrier than the consecutive losses of H_2O + CO.[49] By analogy to these results, the $^+H_2N{=}CH_2$ fragment from $[Gly]H^+$ could arise by sequential cleavages of H_2O + CO, progressing from $\mathbf{1a}^+$, as rationalized in Scheme 1.

More information on the mechanism of $^+H_2N{=}CH_2$ formation is revealed by a recent investigation of Kebarle et al., who measured the dissociation threshold of 1^+ using low-energy CAD.[50] Based on this experiment, $^+H_2N{=}CH_2$ (*m/z* 30) is the fragment of least critical energy. The ion $H_2O\cdots{}^+H_2N{=}CH_2$ (*m/z* 48) starts appearing at higher collision energies, showing

(44) Heerma, W.; Kulik, W.; Burgers, P. C.; Terlouw, J. K. *Int. J. Mass Spectrom. Ion Processes* **1988**, *84*, R1-R5.
(45) Lias, S. G.; Bartmess, J. E.; Liebman, J. F.; Holmes, J. L.; Levin, R. D.; Mallard, W. G. *J. Phys. Chem. Ref. Data* **1988**, *17*, Suppl. No. 1.
(46) Drewello, T.; Heinrich, N.; Maas, W. P. M.; Nibbering, N. M. M.; Weiske, T.; Schwarz, H. *J. Am. Chem. Soc.* **1987**, *109*, 4810–4818.
(47) The relative intensity of $^+H_2NCH_2$ in the MI spectrum of 1^+ remained fairly constant over a period of several months, in which the background pressure ranged between 4.3 × 10^{-8} and 1.1 × 10^{-7} mbar. This result points out that $^+H_2NCH_2$ is largely generated from metastable 1^+, not via CAD with background gases.
(48) (a) Wiedmann, F. A.; Cai, J.; Wesdemiotis, C. *Rapid Commun. Mass Spectrom.* **1994**, *8*, 804–807. (b) Burgers, P. C.; McGibbon, G. A.; Terlouw, J. K. *Chem. Phys. Lett.* **1994**, *224*, 539–543.
(49) Bouchoux, G.; Bourcier, S.; Hoppilliard, Y.; Mauriac, C. *Org. Mass Spectrom.* **1993**, *28*, 1064–1072.
(50) Klassen, J. S.; Anderson, S. A.; Blades, A. T.; Kebarle, P. Presented at the 43rd ASMS Conference on Mass Spectrometry and Allied Topics, Atlanta, GA, May 21–26, 1995, TPA 005.

Table 1. MI Spectra of Ions 1^+-4^+ [a]

ion (*m/z*)	ionization	region	*m/z* 54	52	50	48	34	32	30
$[H_2NCH_2COOH]H^+$, 1^+ (*76*)	CI	FFR-3				100			8
	FAB	FFR-3				100			8
$[H_2NCD_2COOH]H^+$, 2^+ (*78*)	FAB	FFR-3			100			8	
$[D_2NCH_2COOD]D^+$, 3^+ (*80*)	FAB	FFR-3		100				5	
$[D_2NCD_2COOD]D^+$, 4^+ (*82*)	FAB	FFR-3	100				4		

[a] Relative abundance (from peak areas) in % of base peak.

that at threshold *m/z* 30 is not formed from *m/z* 48 via the sequential dissociation $\mathbf{1a}^+ \rightarrow$ *m/z* 48 + CO → *m/z* 30 + CO + H_2O. Kebarle's data support the mechanism of Scheme 1, in which H_2O is eliminated first. The initial H_2O cleavage, proceeding through rearrangement of $\mathbf{1a}^+$ to $H_2NCH_2C(=O)$-OH_2^+ (HO-protonated Gly), produces the α-amino acylium ion $H_2N-CH_2-C\equiv O^+$ (*m/z* 58). Such cations (of class b_1 according to peptide ion fragmentation nomenclature)[1,2] undergo facile exothermic loss of CO[17,33,49] which would lead to the observed immonium ion (*m/z* 30) and explain the absence of an *m/z* 58 peak in Figure 1.[51]

The critical energy needed to generate $^+H_2N{=}CH_2$ (192 kJ mol^{-1})[50] sets the transition state of the reaction $\mathbf{1a}^+ \rightarrow$ $^+H_2N{=}CH_2 + H_2O + CO$ at 446 kJ mol^{-1} (Scheme 1). Since this energy level lies 74 kJ mol^{-1} below $\Delta H_f°(^+H_2N{=}CH_2 + :C(OH)_2)$, the direct cleavage $\mathbf{1b}^+ \rightarrow {}^+H_2N{=}CH_2 + :C(OH)_2$ is ruled out on energetic grounds, at least for metastable precursor ions, whose narrow internal energy distribution (≤50 kJ mol^{-1}) permits only dissociations of quite similar energy demand.[52] The latter property of metastable ions also gives an upper limit for the barrier of the competing channel $\mathbf{1a}^+ \rightarrow H_2O\cdots{}^+H_2N{=}CH_2$ (≤242 kJ mol^{-1}), placing the corresponding transition state at ≤496 kJ mol^{-1}.

The MI spectrum of $\mathbf{1}^+$ does not depend on the ionization mode (FAB or CI), indicating that the same ion(s) is formed regardless of the method used. The isotopomers $\mathbf{2}^+-\mathbf{4}^+$ show parallel behavior (Table 1), consistent with the proposed mechanism. Note the absence of H/D scrambling in the immonium fragments from $\mathbf{2}^+$ and $\mathbf{3}^+$, in agreement with the non-participation of the $-CH_2-$ group in the H_2O + CO loss. The fact that the production of $^+H_2N{=}CH_2$ can readily be explained from isomer $\mathbf{1a}^+$ does not necessarily rule out that the beam of $[Gly]H^+$ entering the metastable reaction zone contains some $\mathbf{1b}^+$ and that the latter ion loses H_2O + CO by an analogous mechanism, i.e. after prior isomerization to the reacting configuration $H_2NCH_2C(=O)OH_2^+$ (Scheme 1).

Collisionally Activated Dissociation. (a) Ionic CAD Products. Collisional activation of ions $\mathbf{1}^+-\mathbf{4}^+$ opens several new decomposition pathways, giving rise to the CAD spectra of Figure 3. These spectra reflect the structure(s) of stable $[Gly]H^+$ ions, i.e. those formed with insufficient internal energy for spontaneous dissociation.[25] All prominent CAD fragment ions

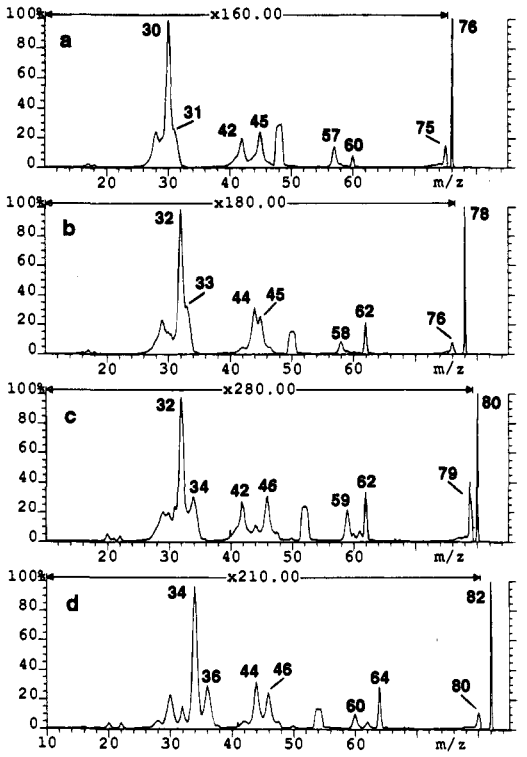

Figure 3. CAD spectra (in FFR-3) of isotopomers $\mathbf{1}^+-\mathbf{4}^+$: (a) $[H_2NCH_2COOH]H^+$, $\mathbf{1}^+$, formed by CH_4-CI (FAB generated $\mathbf{1}^+$ leads to a very similar spectrum); (b) $[H_2NCD_2COOH]H^+$, $\mathbf{2}^+$; (c) $[D_2NCH_2COOD]D^+$, $\mathbf{3}^+$; and (d) $[D_2NCD_2COOD]D^+$, $\mathbf{4}^+$. Ions $\mathbf{2}^+-\mathbf{4}^+$ were formed by FAB.

were studied by MS/MS/MS, in order to assess the unimolecular reactivity of stable protonated glycine and evaluate whether its reactions allow one to pinpoint the site(s) of protonation.

(i) Loss of H•. Ions $[H_2NCD_2COOH]H^+$ ($\mathbf{2}^+$) and $[D_2NCH_2COOD]D^+$ ($\mathbf{3}^+$) cleave D• and H•, respectively, showing that the hydrogen atom eliminated from $[Gly]H^+$ belongs to the methylene group. Depending on the site of protonation in $[Gly]H^+$, such a reaction would produce ylide ion ***a*** or enol ion ***b***.[53] The MS/MS/MS spectrum (Table 2) is dominated by *m/z* 57 (loss of H_2O), which can arise from either ***a*** or ***b***; on the other

hand, the fragments of *m/z* 45 ($^+$COOH) and *m/z* 30 (loss of •COOH) are rather consistent with structure ***a***. Also the relatively abundant doubly charged ion at *m/z* 37.5 is more compatible with an ionized ylide; such ions generally show much higher charge stripping efficiencies than other types of cations.[54,55] The latter data suggest that the H• loss proceeds from $\mathbf{1a}^+$ and generates cation ***a*** (Scheme 2).

(ii) Loss of H• + H_2O. Collisionally excited $\mathbf{1}^+$ gives rise to a fragment at *m/z* 57 which formally emerges by elimination of (H_3,O). The MS/MS/MS spectrum of *m/z* 57 (Table 2) is

(51) The MI spectrum of CI generated $\mathbf{1}^+$ contains no peak at *m/z* 58 (H_2O loss). With FAB produced $\mathbf{1}^+$, a narrow *m/z* 58 signal is observed and originates from the glycerol matrix (H_2O loss from $^{13}CC_2H_5O_2^+$, which is isobaric with $\mathbf{1}^+$). Expectedly, the deuterated isotopomers $\mathbf{2}^+-\mathbf{4}^+$ show no MI fragment corresponding to water loss. Also, *m/z* 58 is absent when thioglycerol or other matrices are used, although now other artefact peaks appear. Overall, glycerol leads to the least background peaks and was, therefore, the preferred FAB matrix for the glycine samples investigated.

(52) The peak width of the $^+H_2N{=}CH_2$ signal corresponds to $T_{0.5}$ = 134 meV (assuming that the complementary neutral loss is cleaved as one piece of 46 u).[26] This $T_{0.5}$ differs markedly from the value expected for the continuously endothermic direct cleavage $\mathbf{1b}^+ \rightarrow {}^+H_2N{=}CH_2 + :C(OH)_2$ (<20 meV),[26] further validating the mechanism of Scheme 1.

(53) Depke, G.; Heinrich, N.; Schwarz, H. *Int. J. Mass Spectrom. Ion Processes* **1984**, *62*, 99–117.

(54) For the charge-stripping spectra of ylide ions see: (a) Holmes, J. L.; Lossing, F. P.; Terlouw, J. K.; Burgers, P. C. *J. Am. Chem. Soc.* **1982**, *104*, 2931–2932. (b) Sack, T. M.; Cerny, R. L.; Gross, M. L. *J. Am. Chem. Soc.* **1985**, *107*, 4562–4564. (c) Wesdemiotis, C.; Feng, R.; Danis, P. O.; Williams, E. R.; McLafferty, F. W. *J. Am. Chem. Soc.* **1986**, *108*, 5847–5853.

(55) For comparison, the abundance of $C_2H_4O_2^{2+}$ (*m/z* 30) in the CAD (O_2) spectrum of enol ion $CH_2{=}C(OH)_2^{+\bullet}$ (***d***) is <1% of [base peak].

Table 2. Partial MS/MS/MS Spectra of Fragment Ions from 1^+–4^+

m/z from ion	fragment ions[a]				structure most consistent with MS/MS/MS fragments and reported ref spectra
***75* from 1^+** [b]	*57*(100)	*45*(10), *37.5*(6)	*30*(13), *29*(21), *28*(19)		$^+H_3N-CH^{\bullet}-COOH$
***60* from 1^+** [b]		*45*(30), *42*(100)	*31*(8), *29*(12)	*15*(2), *14*(2)	$CH_2=C(OH)_2^{\bullet+}$
***57* from 1^+**		*41*(28)	*29*(100), *28*(56)		$^{+\bullet}H_2N-CH=CO$
58 from 2^+		*42*(30)	*30*(100), *29*(57), *28*(30)		$^{+\bullet}H_2N-CD=CO$
59 from 3^+		*41*(25)	*31*(100), *30*(20), *29*(26)		$^{+\bullet}D_2N-CH=CO$
***48* from 1^+**			*30*(100)	*19*(1), *18*(1)	$H_2O\cdots{}^+H_2N=CH_2$
50 from 2^+			*32*(100)	*19*(1), *18*(1)	$H_2O\cdots{}^+H_2N=CD_2$
52 from 3^+			*32*(100)	*22*(2), *20*(1)	$D_2O\cdots{}^+D_2N=CH_2$
54 from 4^+			*34*(100)	*22*(1), *20*(1)	$D_2O\cdots{}^+D_2N=CD_2$
***45* from 1^+**		*44*(100)	*29*(42), *28*(26)	*17*(3)	$COOH^+$
45 from 2^+		*44*(100)	*29*(25), *28*(18)	*17*(3)	$COOH^+$
46 from 3^+		*44*(100)	*30*(55), *28*(45)	*18*(5)	$COOD^+$
46 from 4^+		*44*(100)	*30*(36), *28*(25)	*18*(5)	$COOD^+$
***42* from 1^+**		*41*(100), *40*(15)	*29*(10), *28*(10)	*14*(15)	$CH_2=C=O^{\bullet+}$
44 from 2^+		*42*(100), *40*(11)	*30*(15), *28*(25)	*16*(10)	$CD_2=C=O^{\bullet+}$
42 from 3^+		*41*(100), *40*(18)	*29*(9), *28*(9)	*14*(3)	$CH_2=C=O^{\bullet+}$
44 from 4^+		*42*(100), *40*(14)	*30*(15), *28*(18)	*16*(9)	$CD_2=C=O^{\bullet+}$
***31* from 1^+**			*30*(100), *29*(47), *28*(17)	*17*(1),[c] *14*(1)	$^+H_3N-CH_2^{\bullet}$
33 from 2^+			*32*(100), *31*(60), *30*(28), *29*(22), *28*(8)	*17*(2),[c] *16*(2)	$^+H_3N-CD_2^{\bullet}$
34 from 3^+			*33*(100), *32*(43), *31*(9), *30*(11), *29*(11)	*20*(2)[c]	$^+D_3N-CH_2^{\bullet}$
36 from 4^+			*34*(100), *32*(8), *30*(16)	*20*(1)[c]	$^+D_3N-CD_2^{\bullet}$
***30* from 1^+**			*29*(82), *28*(100), *27*(16)	*16*(1), *14*(1)	$^+H_2N=CH_2$
32 from 2^+			*31*(29), *30*(80), *29*(100), *28*(18), *27*(9)	*16*(2)	$^+H_2N=CD_2$
32 from 3^+			*31*(100), *30*(36), *29*(69), *28*(14), *27*(4)	*18*(2), *14*(1)	$^+D_2N=CH_2$
34 from 4^+			*32*(95), *30*(100), *28*(13), *26*(2)	*18*(2), *16*(2)	$^+D_2N=CD_2$

[a] *m/z* values followed by relative abundances (measured as peak heights) in parentheses. [b] Precursor ions 1^+ generated by CI; in all other cases, the precursor ions were produced by FAB. [c] All isotopomers show $C(H,D)_5N^{2+}$ dications with ~2% relative abundance, consistent with the ylide structure.

Scheme 2

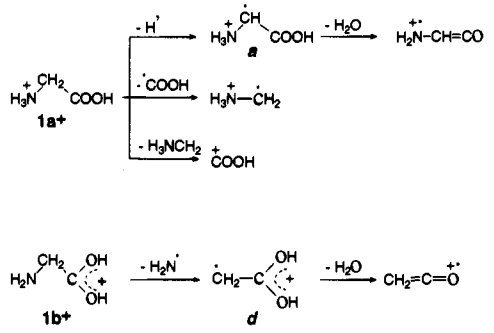

dominated by ions at *m/z* 41 ($H_2N^{\bullet}$ loss) and 29 (CO loss), pointing out the connectivity $^{+\bullet}H_2N-CH=CO$. Similarly, isotopomers 2^+ and 3^+ generate $^{+\bullet}H_2N-CD=CO$ and $^{+\bullet}D_2N-CH=CO$, respectively (based on Table 2). These fragments most likely originate by consecutive water elimination from the primary fragment ***a*** (Scheme 2).

(iii) Loss of $H_2N^{\bullet}$. The fragment ion at *m/z* 60 nominally arises by elimination of 16 mass units. Isomers 2^+, 3^+, and 4^+ rupture to give neutrals of 16, 18, and 18 u, respectively (Figure 3), indicating that this reaction involves the breakup of an amino radical, viz $1^+ \rightarrow H_2N^{\bullet} + C_2H_4O_2^{\bullet+}$. The two $C_2H_4O_2^{\bullet+}$ isomers most feasible from $[Gly]H^+$ are ionized acetic acid (***c***) and its thermodynamically more stable enol (***d***). These species can readily be distinguished from their CAD spectra; ion ***c*** primarily fragments to $CH_3C{\equiv}O^+$ (*m/z* 43) + $^{\bullet}OH$ while ion ***d*** predominantly yields $CH_2=C=O^{\bullet+}$ (*m/z* 42) + H_2O.[56] The MS/MS/MS spectrum of the $C_2H_4O_2^{\bullet+}$ product from 1^+ (Table 2) is dominated by $C_2H_2O^{\bullet+}$ (*m/z* 42) and overall matches the reference spectrum of ion ***d***. Thus, loss of $H_2N^{\bullet}$ from 1^+ produces the enol ion of acetic acid. Such a fragmentation is characteristic for O-protonated glycine, $\mathbf{1b}^+$, which can give $H_2N^{\bullet}$ + ***d*** by a simple N-C bond cleavage (Scheme 2).

(iv) Loss of $H_2N^{\bullet}$ + H_2O. The CAD spectrum of 1^+ (Figure 3a) displays a relatively abundant $C_2H_2O^{\bullet+}$ fragment (*m/z* 42) whose MS/MS/MS spectrum (Table 2) is consistent with the structure of ionized ketene, $CH_2=C=O^{\bullet+}$.[56] This product could arise by successive decomposition of fragment ***d***, whose favored dissociation indeed produces $CH_2=C=O^{\bullet+}$ (see above section). Overall, 1^+ loses $H_2N^{\bullet}$ + H_2O to yield the ketene radical cation (Scheme 2). Isotopomers 2^+ and 3^+ generate solely $CD_2=C=O^{\bullet+}$ and $CH_2=C=O^{\bullet+}$, respectively (Table 2), corroborating that the elimination of $H_2N^{\bullet}$ + H_2O involves exclusively the "acidic" hydrogens attached to the heteroatoms of $[Gly]H^+$.

(v) Loss of CO. The CH_6NO^+ ion arising by CO elimination has been discussed in detail in the MI section. CH_6NO^+ from collisionally activated 1^+ and CH_6NO^+ from metastable 1^+ give rise to identical MS/MS/MS spectra (Figure 2), verifying that the same fragment ion is formed in both processes, namely $H_2O\cdots{}^+H_2N=CH_2$. As mentioned earlier, the formation of such an ion/dipole complex by CO loss is best rationalized from N-protonated glycine, $\mathbf{1a}^+$, which includes an intact C=O substructure (Scheme 1).[57]

(vi) Loss of $^{\bullet}COOH$ and Formation of ^+COOH. Precursors 1^+ and 2^+ eliminate a $^{\bullet}CO_2H$ radical to form fragment ions at *m/z* 31 ($CH_5N^{\bullet+}$) and 33 ($CH_3D_2N^{\bullet+}$), respectively (Figure 3). From the isotopomers 3^+ and 4^+, a $^{\bullet}CO_2D$ radical is lost giving rise to fragments of *m/z* 34 ($CH_2D_3N^{\bullet+}$) and 36 ($CD_5N^{\bullet+}$),

(56) Schwarz, H.; Williams, D. H.; Wesdemiotis, C. *J. Am. Chem. Soc.* **1978**, *100*, 7052–7055.

respectively. The complementary product $^+CO_2H$ (from $\mathbf{1}^+$ and $\mathbf{2}^+$) or $^+CO_2D$ (from $\mathbf{3}^+$ and $\mathbf{4}^+$) is also observed with comparable relative abundance. Based on reference CAD spectra of the conventional ion $^{+\bullet}H_2NCH_3$ and the ylide ion $^+H_3NCH_2^\bullet$,[58] our MS/MS/MS spectra of $C(H,D)_5N^{\bullet+}$ (Table 2) correspond to ylide cations; ylide $^+H_3NCH_2^\bullet$ produces upon CAD substantially more $^{+\bullet}H_3N$, $CH_2^{\bullet+}$, and $^{2+}H_3NCH_2$ than the conventional isomer $^{+\bullet}H_2NCH_3$.[58] Concerning the $^+CO_2(H,D)$ fragment from $\mathbf{1}^+-\mathbf{4}^+$, MS/MS/MS (Table 2) reveals the connectivity $O{=}C{=}O(H,D)^+$ (i.e. protonated/deuterated CO_2). Both fragments $^+H_3NCH_2^\bullet$ and ^+COOH are characteristic for the ammonium structure $\mathbf{1a}^+$, from which they can be generated by a direct $C^\alpha-COOH$ bond scission, as shown in Scheme 2.

(vii) Loss of (C,H_2,O_2). Nominal loss of a (C,H_2,O_2) moiety (46 u) from $\mathbf{1}^+$ yields the immonium ion $^+H_2N{=}CH_2$ (*m/z* 30). Although of minor importance for metastable precursor ions (Figure 1), this product becomes the base peak after CAD (Figure 3a). Cations $\mathbf{2}^+$, $\mathbf{3}^+$, and $\mathbf{4}^+$ lead to base peaks at *m/z* 32 (Figure 3b), 32 (Figure 3c), and 34 (Figure 3d) which, together with the MS/MS/MS data of Table 2, points to the generation of $^+H_2N{=}CD_2$, $^+D_2N{=}CH_2$, and $^+D_2N{=}CD_2$ fragments, respectively.

The $^+H_2N{=}CH_2$ ion can arise from N-protonated glycine ($\mathbf{1a}^+$) by the mechanism outlined in Scheme 1, i.e. by consecutive elimination of water and carbon monoxide. CAD may open additional routes to this fragment, e.g., through sequential decomposition of $H_2O{\cdots}{}^+H_2N{=}CH_2$ (*m/z* 48) or $^+H_3NCH_2^\bullet$ (*m/z* 31). However, as mentioned in the MI section, the simplest route to $^+H_2N{=}CH_2$ would be a direct C−C cleavage from O-protonated Gly ($\mathbf{1b}^+$), involving the loss of $:C(OH)_2$. Such a pathway requires a larger critical energy than the sequential H_2O + CO elimination (see Scheme 1) and, therefore, is not preferred by metastable $\mathbf{1}^+$. However, it could occur after collisional activation which can supply the needed internal energy. If the immonium base peak originates via $:C(OH)_2$ loss, then a significant amount of the $[H_2NCH_2COOH]H^+$ precursor ions should have the structure $\mathbf{1b}^+$.[26c] Whether this is true can be found by interrogating the composition of the neutral species cleaved upon CAD of $\mathbf{1}^+$.

(b) Neutral CAD Products. The neutral mixture liberated upon CAD of $[Gly]H^+$ is made detectable by collision induced dissociative ionization (CIDI).[30] During this post-ionization process, each neutral loss generates several ionic products which give rise to a unique CIDI mass spectrum. Superposition of the CIDI spectra of all neutrals co-released from $\mathbf{1}^+$ leads to the ultimately observed neutral fragment-reionization (N_fR)[33,59] mass spectrum of $\mathbf{1}^+$, illustrated in Figure 4 along with the spectra of isotopomers $\mathbf{2}^+-\mathbf{4}^+$.

If the $^+H_2N{=}CH_2$ base peak in the CAD spectrum of $[Gly]H^+$ is the result of dihydroxycarbene elimination from the O-protonated isomer $\mathbf{1b}^+$, then a significant amount of neutral $:C(OH)_2$ should be contained in the neutral loss mixture liberated from $[H_2NCH_2COOH]H^+$. Recent neutralization−reionization studies have shown that the carbene $:C(OH)_2$ is a stable neutral species,[48] inhibited by considerable barriers from isomerization

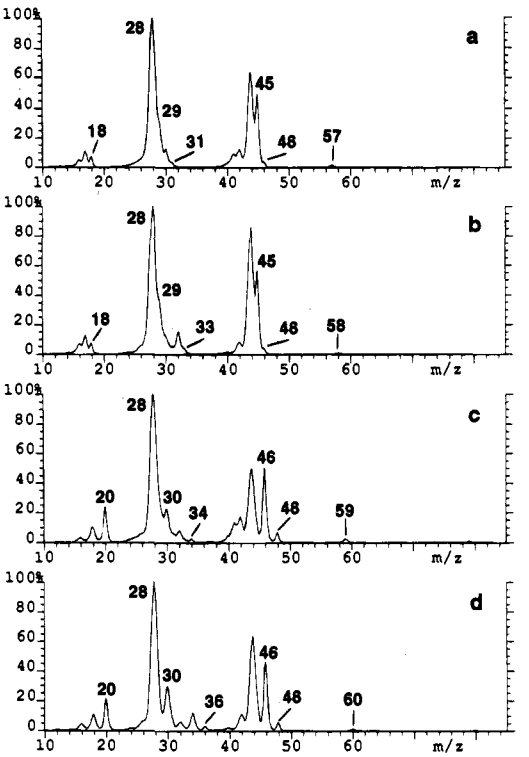

Figure 4. N_fR spectra of isotopomers $\mathbf{1}^+-\mathbf{4}^+$ produced by FAB: (a) $[H_2NCH_2COOH]H^+$, $\mathbf{1}^+$; (b) $[H_2NCD_2COOH]H^+$, $\mathbf{2}^+$; (c) $[D_2NCH_2COOD]D^+$, $\mathbf{3}^+$; and (d) $[D_2NCD_2COOD]D^+$, $\mathbf{4}^+$. The N_fR spectrum of CH_4-CI generated $\mathbf{1}^+$ is identical to that in part a.

to more stable formic acid or from spontaneous dissociation to CO + H_2O or H_2 + CO_2. The reference NR spectrum of $^{+\bullet}C(OH)_2$ contains an abundant recovered precursor ion at *m/z* 46 (recovery peak).[48] Furthermore, the NR yields of $^{+\bullet}C(OH)_2$ and ^+COOH are comparable,[60] warranting that $:C(OH)_2$ and $^\bullet COOH$ are cationized with comparable efficiencies. Therefore, an appreciable amount of $:C(OH)_2$ in the neutral beam eliminated from $\mathbf{1}^+$ (or $\mathbf{2}^+$) should give rise to a sizable recovery signal at *m/z* 46.[27,29] However, the relative abundance of *m/z* 46 ($CH_2O_2^{\bullet+}$) in the N_fR spectra of Figures 4a,b is tiny. Similarly, the N_fR spectra of ions $\mathbf{3}^+$ and $\mathbf{4}^+$ (which would have lost $:C(OD)_2$) display very little *m/z* 48 ($CD_2O_2^{\bullet+}$). Evidently, elimination of complete dihydroxycarbene units is not the major pathway to the $^+(H,D)_2N{=}C(H,D)_2$ ions from $\mathbf{1}^+-\mathbf{4}^+$. For the same reason, the loss of whole HCOOH molecules is also inconsistent with the experimental finding. The N_fR data rather indicate that the immonium base peak must mainly originate from elimination of H_2O + CO, both of which supply major N_fR products (*vide infra*). Expulsion of H_2O + CO can commence from (and thus is characteristic of) N-protonated glycine $\mathbf{1a}^+$, the thermodynamically most stable isomer (see Scheme 1). Nevertheless, the small amount of complete CH_2O_2 moieties observed among the neutral losses from $\mathbf{1}^+$ suggests that a certain (albeit small) amount of O-protonated Gly ($\mathbf{1b}^+$) may also be present in the mass-selected $[Gly]H^+$ beam undergoing CAD.

The base peak in all N_fR spectra is $CO^{\bullet+}$ (*m/z* 28); a large fraction of this ion must originate from CIDI of CO, coproduced with the $H_2O{\cdots}{}^+H_2N{=}CH_2$ and $^+H_2N{=}CH_2$ fragment ions (Scheme 1). Other important neutral losses that are readily identifiable from the N_fR data are H_2O/D_2O and $^\bullet COOH/^\bullet COOD$ (see Schemes 1 and 2). Water is the main contributor of the

(57) The absolute abundance of the peak for CO loss (*m/z* 48) becomes larger as small and then increasing amounts of collision gas are admitted. Such a result supports the mechanism of Scheme 1, in which CO is cleaved via a one-step reaction. If CO elimination had been preceded by rearrangement to a stable intermediate, [*m/z* 48] would have remained fairly constant upon collisional activation. See: Levsen, K. *Fundamental Aspects of Organic Mass Spectrometry*; Verlag Chemie: Weinheim, 1978.

(58) Holmes, J. L.; Lossing, F. P.; Terlouw, J. K.; Burgers, P. C. *Can. J. Chem.* **1983**, *61*, 2305−2309.

(59) Cordero, M. M.; Wesdemiotis, C. In *Biological Mass Spectrometry: Present and Future*, Caprioli, R., Gross, M. L., Matsuo, T., Seyama, Y., Eds.; John Wiley & Sons, Ltd.: Chichester, 1994; pp 119−126.

(60) The NR yields of ^+COOH and $^{+\bullet}C(OH)_2$ (total ion flux in NR spectrum divided by unattenuated main beam flux) are 5 × 10^{-4} and 1 × 10^{-3}, respectively.

$H_{0-2}O^+$ and $D_{0-2}O^+$ peaks in Figures 4a,b and 4c,d, respectively.[61] On the other hand, radicals •COOH and •COOD are the principal source of $^+$COOH (*m/z* 45)/$[H,C,O]^+$ (29) and $^+$COOD (*m/z* 46)/$[D,C,O]^+$ (30) in Figures 4a,b and 4c,d, respectively, and of $CO_2^{\bullet+}$ and $CO^{\bullet+}$ in all four N_fR spectra.[62]

The N_fR spectrum of $\mathbf{1}^+$ includes a small peak at *m/z* 31, which shifts to *m/z* 33 for $\mathbf{2}^+$, *m/z* 34 for $\mathbf{3}^+$, and *m/z* 36 for $\mathbf{4}^+$, thereby revealing the composition $CH_5N^{\bullet+}$. This ion can result from the CH_5N loss accompanying the $^+$COOH fragment (see Scheme 2), which in turn could be H_3NCH_2 or H_2NCH_3. Ylide H_3NCH_2 arises from $\mathbf{1a}^+$ by a simple bond cleavage and has been found by theory[63] and experiment[54c] to exist as a stable species. However, once formed, H_3NCH_2 may rearrange to more stable methylamine if the CAD process produces it with enough excitation;[63] the N_fR data do not allow us to determine whether this happened.

Finally, the N_fR products at *m/z* 57 (trace), 42–40, and 30 in the spectrum of $\mathbf{1}^+$ (Figure 4a) most probably arise from Gly,[64] formed via $\mathbf{1}^+ \rightarrow H^+ + Gly$.[65] As the largest neutral loss, Gly has high kinetic energy and therefore superior reionization and transmission efficiency, with the result that it provides a visible contribution to the N_fR spectrum, even if it is a minor component in the neutral loss mixture from $\mathbf{1}^+$.[33-35,66]

According to the combined CAD and N_fR data of $\mathbf{1}^+$–$\mathbf{4}^+$, the majority of $[Gly]H^+$'s fragmentations reflect ammonium structure $\mathbf{1a}^+$. Nevertheless, the small amount of intact CH_2O_2 loss observed and the occurrence of a $H_2N^{\bullet}$ (and $H_2N^{\bullet} + H_2O$) elimination point out that FAB and CI protonation also generate some O-protonated species $\mathbf{1b}^+$, which does not freely isomerize to more stable $\mathbf{1a}^+$.[25,26] This would mean that the interconversion $\mathbf{1b}^+ \rightarrow \mathbf{1a}^+$ must pass over a finite barrier. Alternatively, our experimental observations could be explained by assuming that only $\mathbf{1a}^+$ is formed upon ionization but that some of its CAD reactions proceed after prior collision induced isomerization to $\mathbf{1b}^+$.[25,26] The ionic and neutral dissociation products of cation $\mathbf{1}^+$ cannot differentiate between these two cases. Therefore, more information on this topic was sought by inquiring into the unimolecular stability and reactivity of $\mathbf{1}^+$'s neutralized form(s). While $\mathbf{1a}^+$ and $\mathbf{1b}^+$ may need less energy to interconvert than to dissociate, this should not be true for the corresponding neutrals **1a** and **1b**, which are dramatically different in their bonding and stability.

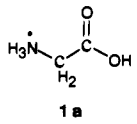

1a

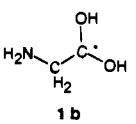

1b

Unimolecular Chemistry of Neutralized $[Gly]H^+$. (a) Ammonium Radical 1a. Radical **1a** contains a nitrogen atom surrounded by nine valence electrons, which violates the octet rule making **1a** hypervalent.[67] Hypervalent ammonium radicals of the type $^{\bullet}H_3N-R$ have extremely short lifetimes for experimental observation (<0.1 μs), unless stabilization is incurred at the hypervalent center by complete deuteration or by clustering.[68] A plain $^{\bullet}H_3N-R$ radical is separated by minuscule barriers from dissociation to more stable products.[68] If formed by vertical neutralization of a keV $^+H_3N-R$ cation, $^{\bullet}H_3N-R$ emerges in the geometry of $^+H_3N-R$ and not in the $^{\bullet}H_3N-R$ ground state; this excitation leads to complete unimolecular decay, so that no recovered precursor ion is observed after reionization.[68b] Based on the reported $^{\bullet}H_3N-R$ reactivities,[68] ammonium radical **1a** should decompose upon its formation by simple bond cleavages to yield bound neutral fragments, as shown in Scheme 3.

Scheme 3[a]

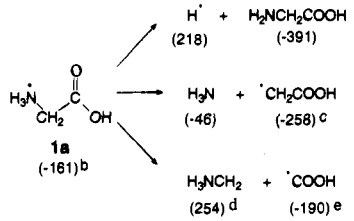

[a] All numbers given are $\Delta H_f°$ values in kJ mol^{-1} from ref 45 (unless otherwise noted). [b] $\Delta H_f°(\mathbf{1a}) = \Delta H_f°(\mathbf{1a}^+)$ (see Scheme 1) − IE(**1a**). It is presumed that IE(**1a**) ≈ IE($^{\bullet}H_3NCH_3$) = 4.3 eV.[68b] [c] Reference 69. [d] Estimated from $\Delta H_f°(H_2NCH_3) = -23$ kJ mol^{-1} [45] and the theoretically calculated energy difference between H_2NCH_3 and H_3NCH_2.[63] [e] Reference 62.

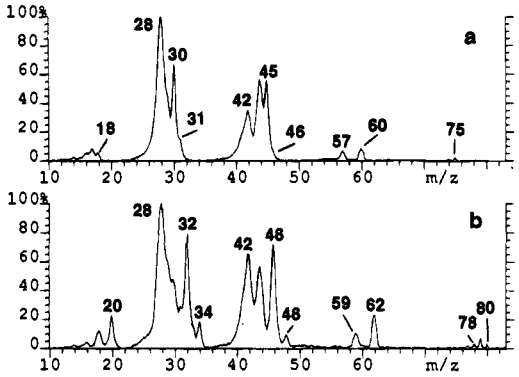

Figure 5. NR spectra of isotopomers $\mathbf{1}^+$ and $\mathbf{3}^+$ produced by FAB: (a) $[H_2NCH_2COOH]H^+$, $\mathbf{1}^+$; and (b) $[D_2NCH_2COOD]D^+$, $\mathbf{3}^+$. The NR spectrum of CH_4-CI generated $\mathbf{1}^+$ is identical to that in part a.

The fragments H_2NCH_2COOH (Gly), H_3NCH_2, and •COOH from **1a** (Scheme 3), for which CIDI or NR spectra have been published,[54c,62,64] are readily detected in the NR spectrum of $\mathbf{1}^+$ (Figure 5a). Gly mainly contributes to *m/z* 75–74 ($M^{\bullet+}$ and $[M - H]^+$), 57 ($^+{}^{\bullet}H_2NCHCO$), 45 ($^+$COOH), 42 ($C_2H_2O^{\bullet+}$), 30 ($^+H_2N{=}CH_2$), and 28.[64] Radical •COOH gives rise to major peaks at *m/z* 45–44 ($^+$COOH and $CO_2^{\bullet+}$), 29 ($[H,C,O]^+$), and 28 ($CO^{\bullet+}$).[62] And ylide H_3NCH_2 primarily provides ions of *m/z* 31–26 ($CH_{5-0}N^+$), from which *m/z* 31 ($M^{\bullet+}$) is clearly discernable;[54c] as noticed earlier, the same ions would arise if H_3NCH_2 isomerized to the more stable H_2NCH_3 molecule prior to reionization.

(61) For the CIDI spectrum of H_2O see: Burgers, P. C.; Holmes, J. L.; Mommers, A. A.; Szulejko, J. E.; Terlouw, J. K. *Org. Mass Spectrom.* **1984**, *19*, 442–447.

(62) For the NR spectrum of $^+$COOH see: Holmes, J. L.; Mommers, A. A.; Terlouw, J. K.; Hop, C. E. C. A. *Int. J. Mass Spectrom. Ion Processes* **1986**, *68*, 249–264.

(63) Yates, B. F.; Bouma, W. J.; Radom, L. *J. Am. Chem. Soc.* **1987**, *109*, 2250–2263.

(64) The CIDI (O_2) spectrum of 4 keV Gly, produced via dissociation of the proton-bound dimer, shows peaks at *m/z* 28 (53%), 30 (100%), 40–42 (25%), 45 (59%), 57 (4%), 74 (7%), and 75 (3%). Reducing the kinetic energy increases the relative abundances of *m/z* >45 and vice versa; see: Cordero, M. M.; Wesdemiotis, C. *Org. Mass Spectrom.* **1994**, *29*, 382–390.

(65) With isotopomers $\mathbf{2}^+$, $\mathbf{3}^+$, and $\mathbf{4}^+$, these products appear at *m/z* 58, 44–40, and 32 (for $\mathbf{2}^+$), at *m/z* 59, 42–40, and 32 (for $\mathbf{3}^+$), and at *m/z* 60, 44–40, and 34 (for $\mathbf{4}^+$), in line with the connectivities $^{+\bullet}(H,D)_2N-C(H,D){=}CO$, $C(H,D)_{2-0}{=}C{=}O^{\bullet+}$, and $^+(H,D)_2N{=}C(H,D)_2$, respectively.

(66) Li, X.; Harrison, A. G. *J. Am. Chem. Soc.* **1993**, *115*, 6327–6332.

(67) Schleyer, P. v. R. In *New Horizons in Quantum Chemistry*; Löwdin, P.-O., Pullman, B., Eds.; Reidel: Dodrecht, 1983; p 95.

(68) (a) Gellene, G. I.; Cleary, D. A.; Porter, R. F. *J. Chem. Phys.* **1982**, *77*, 3471–3477. (b) Jeon, S.-J.; Raksit, A. B.; Gellene, G. I.; Porter, R. F. *J. Am. Chem. Soc.* **1985**, *107*, 4129–4133.

(69) Holmes, J. L.; Lossing, F. P.; Mayer, P. M. *J. Am. Chem. Soc.* **1991**, *113*, 9723–9728.

The thermodynamically most stable product combination from **1a**, namely H_3N + $^{\bullet}CH_2COOH$ (Scheme 3), is more difficult to uncover in the NR spectrum of $[Gly]H^+$ (Figure 5a). $H_3N^{\bullet+}$ (*m/z* 17) overlaps with HO^+ (from reionization of H_2O, *vide infra*); and for $^{\bullet}CH_2COOH$ (59 u), no reference spectrum is available. The absence of a recognizable *m/z* 59 signal in Figure 5a suggests that H_3N + $^{\bullet}CH_2COOH$ are not important dissociation products of **1a**.[70] Interestingly, the well-studied hypervalent ammonium radical $^{\bullet}H_3NCH_3$ shows a parallel behavior;[68a] it primarily (>80%) decomposes to $H^{\bullet}$ + H_2NCH_3 ($\sum\Delta H_f^\circ$ = 195 kJ mol^{-1}),[45] not to the more stable products H_3N + $^{\bullet}CH_3$ (100 kJ mol^{-1}).[45] Gellene et al. proposed that H_3N loss from $^{\bullet}H_3NCH_3$ is discriminated against by a higher barrier;[68] this may be the case for **1a**, too.

The NR spectrum of $\mathbf{1}^+$ contains certain ions that cannot be reconciled with radical **1a**. Among them are the products of *m/z* 18 ($H_2O^{\bullet+}$) and 60 ($C_2H_4O_2^{\bullet+}$, i.e. $[\mathbf{1}-H_2N^{\bullet}]^{\bullet+}$). Such ions cannot originate from the neutral fragments of **1a** shown in Scheme 3. H_2O or $H_2N^{\bullet}$ loss from **1a** itself also is unlikely; as an unstable species, this hypervalent radical should not live long enough to allow for the rearrangements needed for H_2O or $H_2N^{\bullet}$ cleavage.

The H_2O observed in the NR spectrum of $[Gly]H^+$ might be due to the trimethylamine (TMA) target used for neutralization (Figure 5) causing some concomitant CAD of precursor ion $\mathbf{1}^+$, which does liberate water (see CAD section). Several arguments speak however against such a situation: (i) TMA is a superior neutralization target with relatively low dissociation and high charge exchange efficiency.[43,72] (ii) The peak width of $H_2O^{\bullet+}$ (and of the other fragments) in the NR spectrum of Figure 5a is substantially larger than the peak width of $H_2O^{\bullet+}$ in the N_fR spectrum of Figure 4a, where the water *is* formed by CAD (i.e. via $\mathbf{1}^+ \rightarrow H_2O$). The greater kinetic energy release observed in the NR spectrum is rather consistent with formation of H_2O from an excited neutral (i.e. via $\mathbf{1}^+ \rightarrow \mathbf{1}^* \rightarrow H_2O$).[29,68] Many other neutral dissociations have been demonstrated to proceed with a larger kinetic energy release than the corresponding ionic dissociations.[27,29,41a,68,72] Based on these factors, we conclude that the ions observed in Figure 5a primarily result from the neutral intermediate **1**, not through CAD of cation $\mathbf{1}^+$.

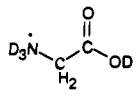

3a

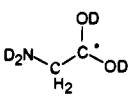

3b

Analogous results are obtained from the other isotopomers, of which $\mathbf{3}^+$ is presented in Figure 5b. Many important fragments in this spectrum can be explained as arising from the ammonium radical **3a**, after decomposition of the latter to $D^{\bullet}$ + D_2NCH_2COOD and D_3NCH_2 + $^{\bullet}COOD$ (viz Scheme 3).

Scheme 4[a]

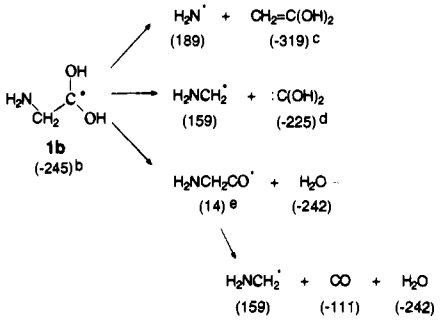

[a] See Scheme 3. [b] Estimated from $\Delta H_f^\circ(CH_3CH_2C(OH)_2^{\bullet})$ = −302 kJ mol^{-1},[73] using Benson's group equivalents.[74] [c] Reference 73. [d] Reference 48a. [e] Estimated from $\Delta H_f^\circ(CH_3CH_2CO^{\bullet})$ = −43 kJ mol^{-1},[45] using Benson's group equivalents.[74]

Reionization of D_2NCH_2COOD leads primarily to $^{+\bullet}D_2NCHCO$ (*m/z* 59), ^+COOD (46), $C_2H_2O^{\bullet+}$ (42), and $^+D_2NCH_2$ (32); some $M^{\bullet+}$ (*m/z* 78) and $[M - H]^+$ (77) are also observed. D_3NCH_2 and $^{\bullet}COOD$ mainly produce $CH_{2-0}D_{3-0}N^+$ (*m/z* 34−26) and ^+COOD (*m/z* 46)/$CO_2^{\bullet+}$ (44)/$[D,C,O]^+$ (30)/$CO^{\bullet+}$ (28), respectively. It is noteworthy that the NR spectrum of $\mathbf{3}^+$ contains a small recovered precursor ion ("survivor" ion) at *m/z* 80, pointing out that, in contrast to **1a**, hypervalent radical **3a** (which is perdeuterated at the ammonium center) can survive intact. Gellene et al. reported similar stability for the related radicals $^{\bullet}D_4N$ and $^{\bullet}D_3NCH_3$.[68] Notice that reionization of **3a** mainly causes $H^{\bullet}$, not $D^{\bullet}$, loss in accord with the behavior of collisionally activated $\mathbf{3a}^+$ (Figure 5b vs Figure 3c).

As with isotopomer $\mathbf{1}^+$, certain ions in the NR spectrum of $\mathbf{3}^+$ (Figure 5b) are not compatible with **3a** being the only incipient neutralization product. This is true for $D_2O^{\bullet+}$ (*m/z* 20), $CD_2O_2^{\bullet+}$ (*m/z* 48, possibly $^{+\bullet}C(OD)_2$), and $C_2H_2D_2O_2^{\bullet+}$ (*m/z* 62, i.e. $[\mathbf{3}-D_2N^{\bullet}]^{\bullet+}$). These products and the corresponding ones from $\mathbf{1}^+$ (*vide supra*) could arise from isomer **1b** (or **3b**), as rationalized in Scheme 4 for the nondeuterated species.

(b) Dihydroxyalkyl Radical 1b. Radical **1b** is not hypervalent and may be a bound species (see below). Cleavage of $H_2N^{\bullet}$ from **1b** accounts for the $[\mathbf{1}-H_2N^{\bullet}]^{\bullet+}$ ion (*m/z* 60) in the NR spectrum of $\mathbf{1}^+$ (Figure 5a). This ion can originate from dissociation of neutral **1b**, as shown in Scheme 4, or from dissociation after reionization, i.e. via $\mathbf{1b} \rightarrow \mathbf{1b}^+ \rightarrow H_2N^{\bullet}$ + $C_2H_4O_2^{\bullet+}$ (*m/z* 60). The same processes yield $[\mathbf{3}-D_2N^{\bullet}]^{\bullet+}$ (*m/z* 62) from isotopomer **3b** (Figure 5b).[75]

Breakup of the $C-C(OH)_2$ bond in **1b** or of the $C-C(OD)_2$ bond in **3b** can rationalize the peaks at *m/z* 46 ($CH_2O_2^{\bullet+}$, nonresolved shoulder) and 48 ($CD_2O_2^{\bullet+}$), respectively, in the NR spectra of Figures 5a and 5b. Again, the neutral radicals may dissociate before reionization (as illustrated for **1b** in Scheme 4) and/or after reionization. In both cases, $^+H_2NCH_2$ of *m/z* 30 (from **1b**) and $^+D_2NCH_2$ of *m/z* 32 (from **3b**) are cogenerated; these latter ions do appear in the NR spectra (Figure 5) but, as discussed in the previous section, are also produced from the ammonium radicals **1a** and **3a**.

Elimination of H_2O from radical **1b** necessitates rearrangement. Since **1b** is not hypervalent, it ought to live sufficiently long to permit this reaction.[76] The released H_2O must be the source of $H_{2-0}O^+$ (*m/z* 18−16) in the NR spectrum of $\mathbf{1}^+$ (Figure

(70) Reionization of $^{\bullet}CH_2COOH$ would yield the primary carbenium ion $^+CH_2COOH$ (*m/z* 59). This cation, when generated by electron ionization of iodoacetic acid,[71] has been shown to collapse to the more stable ring-closed form *cyclo*-$CH_2-O-C^+(OH)$. The corresponding CAD spectrum, which may represent an approximate reference spectrum of the $^{\bullet}CH_2COOH$ radical, contains (*inter alia*) an abundant *m/z* 58 fragment that is absent in Figure 5a, in keeping with the conclusion that no measurable amount of $^{\bullet}CH_2COOH$ is formed from **1a**.

(71) Blanchette, M. C.; Holmes, J. L.; Hop, C. E. C. A.; Lossing, F. P.; Postma, R.; Ruttink, P. J. A.; Terlouw, J. K. *J. Am. Chem. Soc.* **1986**, *108*, 7589−7594.

(72) Beranová, Š.; Wesdemiotis, C. *Int. J. Mass Spectrom. Ion Processes* **1994**, *134*, 83−102.

(73) Espinosa-Garcia, J.; Olivares del Valle, F. J.; Leroy, G.; Sana, M. *THEOCHEM* **1992**, *258*, 315−330.

(74) (a) Benson, S. W. *Thermochemical Kinetics*, 2nd ed.; Wiley Interscience: New York, 1976. (b) Cohen, N.; Benson, S. W. *Chem. Rev.* **1993**, *93*, 2419−2438.

(75) The kinetic energies released ($T_{0.5}$) during the formation of $[\mathbf{3}-D_2N^{\bullet}]^{\bullet+}$ on CAD and NR are 43 (Figure 3c) and 243 meV (Figure 5b), respectively. The substantially larger value observed for the latter process suggests that, in the NR experiment, $D_2N^{\bullet}$ is rather eliminated from the neutral intermediate, not after reionization.[27,29,41a,68,72] The same is true for $[\mathbf{1}-H_2N^{\bullet}]^{\bullet+}$ (viz. Figure 3a vs Figure 5a).

(76) Wentrup, C. *Reactive Molecules: The Neutral Reactive Intermediates in Organic Chemistry*; Wiley Interscience: New York, 1984.

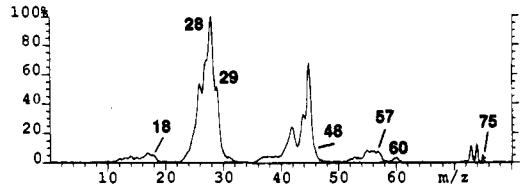

Figure 6. NR spectrum of $CH_3CH_2C(OH)_2^+$, $\mathbf{5}^+$, produced by CH_4-CI.

5a). Similarly, the D_2O molecules eliminated from isotopomer **3b** give rise to the $D_{2-0}O^+$ peaks (*m/z* 20−16) in Figure 5b.[77] The fragment emerging from water loss is the aminoacetyl radical, $H_2NCH_2CO^\bullet$ (Scheme 4). Its reionized form, i.e. $H_2NCH_2CO^+$ (*m/z* 58), is unstable and dissociates to $^+H_2NCH_2$ (*m/z* 30) + CO (see MI section), thus explaining the absence of *m/z* 58 in Figure 5a (or of *m/z* 60 in Figure 5b). It is also quite probable that the weakly bonded $H_2NCH_2CO^\bullet$ radical dissociates itself to $H_2NCH_2^\bullet$ + CO prior to reionization (Scheme 4).

In order to substantiate that the reactions depicted in Scheme 4 are characteristic for dihydroxy substituted alkyl radicals, we also investigated the closely related radical **5** which is the neutral

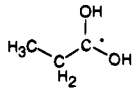

5

counterpart of protonated propanoic acid, $\mathbf{5}^+$ (*m/z* 75). The NR spectrum of $\mathbf{5}^+$ (Figure 6) includes a recovery peak at *m/z* 75, confirming that C-centered radicals carrying an alkyl and two hydroxyl groups can be stable species. Note, however, that [*m/z* 75] is very small suggesting extensive dissociation of **5** before and/or after reionization. For **1b**, which is coproduced with the unstable radical **1a**, an even smaller survivor ion should appear after NR. In addition, the primary amine group in **1b** may promote dissociation upon reionization. This expectation is drawn out of the fact that the electron ionization mass spectra of primary amines show very weak (if at all) $M^{\bullet+}$ ions; e.g., $[M^{\bullet+}]$ of glycine (75 u) is <5% of the base peak.[78] Hence, the negligible intensity of the recovery peak in the NR spectrum of $[Gly]H^+$ (Figure 5a) is not at odds with the presence of some **1b** in the neutral mixture emerging upon neutralization of precursor ion $\mathbf{1}^+$.[79]

The NR and CAD spectra of ion $\mathbf{5}^+$ are significantly different from each other,[80] pointing out that a large fraction of radical **5** decomposes within the ~1 μs available between the neutralization and reionization events. Of importance for this study is that the reaction channels of **1** rationalized through structure **1b** (Scheme 4) are observed for the related radical **5**, too (Scheme 5). Specifically, (i) in analogy to the $[\mathbf{1}-H_2N^\bullet]^{\bullet+}$ ion observed in the NR spectrum of $\mathbf{1}^+$ (Figure 5a), the corresponding spectrum of $\mathbf{5}^+$ (Figure 6) includes a sizable $[\mathbf{5}-CH_3^\bullet]^{\bullet+}$ product; both these ions appear at *m/z* 60 ($C_2H_4O_2^{\bullet+}$). (ii) Cleavage of the $C-C(OH)_2$ bond to ultimately generate

Scheme 5[a]

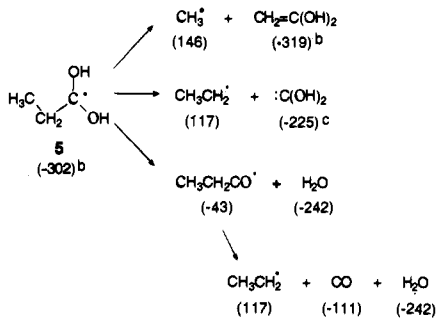

[a] See Scheme 3. [b] Reference 73. [c] Reference 48a.

$CH_2O_2^{\bullet+}$ (*m/z* 46, probably $^{+\bullet}C(OH)_2$) takes place with **1b** as well as with **5**; in both cases the *m/z* 46 peak is a nonresolved shoulder of the more abundant *m/z* 45 signal. (iii) Similar to **1b**, radical **5** loses water, which leads to the $H_{2-0}O^+$ ions (*m/z* 18−16) in the NR spectrum of Figure 6. The propanoyl radical arising after H_2O loss most likely dissociates further to $CH_3CH_2^\bullet$ and CO (Scheme 5), which contribute abundant *m/z* 29−24 and 28 fragments to Figure 6, respectively. This consecutive dissociation explains why the relative abundance of $CH_3CH_2CO^+$ (*m/z* 57) is relatively small after NR.

The described analogies between the NR spectra of $\mathbf{1}^+$ and $\mathbf{5}^+$ provide supporting evidence that the neutral beam emerging from neutralization of $[Gly]H^+$ contains a finite amount of the dihydroxy radical **1b**. For this, O-protonated glycine ($\mathbf{1b}^+$) must have been present in the mass-selected beam leaving the FAB (or CI) ionization region.

According to *ab initio* theory, $\mathbf{1b}^+$ is thermodynamically less stable than $\mathbf{1a}^+$ (by 58−75 kJ mol^{-1}).[10,11,13] Its experimental observation therefore indicates that the intramolecular tautomerization $\mathbf{1b}^+ \rightarrow \mathbf{1a}^+$ has to overcome a considerable barrier. No *ab initio* value is available for this barrier. Semiempirical AM1 calculations,[81] performed in our laboratory using the MOPAC 93 program, predict a critical energy of 77 kJ mol^{-1} for $\mathbf{1b}^+ \rightarrow \mathbf{1a}^+$, corroborating that $\mathbf{1b}^+$ exists as a distinct, stable ion; at the AM1 level, $\mathbf{1b}^+$ is found to lie 36 kJ mol^{-1} above $\mathbf{1a}^+$.

Conclusions

In spite of its small size, protonated glycine ($[Gly]H^+$, $\mathbf{1}^+$) exhibits a rather complex gas phase chemistry. Its spontaneous unimolecular decompositions proceed through tight rearrangements, producing stable ions by loss of small, stable neutrals (Scheme 1). These rearrangements remain favored upon CAD, although now additional, more direct channels are also observed (Scheme 2). In contrast, the reactions of neutralized $[Gly]H^+$ (i.e. of radical **1**) involve simple bond cleavages, leading to bound neutral fragments (Schemes 3 and 4).

$\mathbf{1}^+$'s proclivity for rearrangement makes it very difficult to determine the protonation site of $[Gly]H^+$ based on its unimolecular reactions. This problem arises because the fragments produced from $\mathbf{1}^+$ (ionic or neutral) do not unequivocally reveal whether both $\mathbf{1a}^+$ and $\mathbf{1b}^+$ are formed upon ionization or whether only the more stable ammonium cation $\mathbf{1a}^+$ is formed and later passes through $\mathbf{1b}^+$ upon fragmentation. Theory shows a significant amount of hydrogen bonding in N-protonated glycine;[10] thus H^+ migration should be easily feasible.[82]

The high isomerization tendency of tautomers $\mathbf{1a}^+$ and $\mathbf{1b}^+$ is removed in the corresponding neutrals which, as marginally stable species, prefer direct and structure-diagnostic dissociations. Our NR data show that neutralization of $\mathbf{1}^+$ produces

(77) Note that Figure 5b contains $D_2O^{\bullet+}$ (*m/z* 20) but no $HDO^{\bullet+}$ (*m/z* 19). As pointed out by one reviewer, this result rules out that water is eliminated from isomer **3a**, which could lose HDO via **3a** → $D^\bullet$ + D_2NCH_2COOD → $D^\bullet$ + HDO + $D_2NCH{=}C{=}O$.

(78) McLafferty, F. W.; Stauffer, D. B. *Wiley/NBS Registry of Mass Spectral Data*; Wiley: New York, 1989.

(79) The larger relative intensity of the survivor ion from $\mathbf{3}^+$ (Figure 5b) may be due to both the increased stability of **3b** vs **1b** and, as already mentioned, the greater stability of **3a** vs **1a**.

(80) The CAD (O_2) spectrum of $\mathbf{5}^+$ displays peaks at *m/z* (rel abundance in %): *74* (48), *73* (44), *60* (10), *57* (100), *55* (17), *53* (5), *47* (6), *46* (33), *45* (70), *42* (21), *39*−36 (3; not resolved), *31* (7), *29* (66), *28* (32), *27* (40), *26* (21), *19* (≤1), *18* (<1), *17* (<1), *15* (1), and *14* (1).

(81) Dewar, D. J. S.; Zoebisch, E. G.; Eamonn, F.; Stewart, J. J. P. *J. Am. Chem. Soc.* **1985**, *107*, 3902−2909.

both **1a** and **1b**. Consequently, both tautomers $\mathbf{1a}^+$ and $\mathbf{1b}^+$ are present in the $[Gly]H^+$ beam reaching the neutralization cell. This result means that FAB (and CI) protonation yields both tautomers and that there is an appreciable barrier between them (otherwise $\mathbf{1b}^+$ would collapse to more stable $\mathbf{1a}^+$).[83] Semiempirical MO theory indeed predicts a sizable tautomerization barrier. High-level ab initio data would be most valuable to confirm the magnitude of this barrier.

A notable observation of this study is that protonated glycine ions generated by FAB or CH_4-CI display the same MS/MS spectra (MI, CAD, N_fR, and NR). Such experiments sample long-lived ions (lifetime >12 μs) that did not have sufficient internal energy to decompose before entering the MS/MS reaction zone. Obviously, the structure of these ions does not depend on the method of their formation.

Acknowledgment. We thank the National Institutes of Health and the University of Akron for their generous financial support.

JA950446T

(82) The attempt to produce pure $^+H_3NCH_2COOH$ ($\mathbf{1a}^+$) by an ion–molecule reaction between H_3N and the $[M - I]^+$ ion from iodoacetic acid (ICH_2COOH)[71] was not successful. This reaction generated a mixture of several $C_2H_6NO_2^+$ ions. CI protonation by NH_4^+ was also tried to produce pure $\mathbf{1a}^+$; since the PA of ammonia (853.5 kJ mol^{-1})[45] is considerably higher than that of carboxylic acids (~800 kJ mol^{-1}),[45] ion $\mathbf{1b}^+$ should not be accessible upon reaction of Gly with NH_4^+. However, using NH_3 as the CI reagent did not change markedly the spectra of $[Gly]H^+$. This is attributed to the presence in the CI source of ions other than NH_4^+ (e.g., $NH_3^{\bullet+}$), which can generate $\mathbf{1b}^+$ by exothermic processes. Thus, charge exchange between $NH_3^{\bullet+}$ and Gly (i.e. $NH_3^{\bullet+}$ + Gly → NH_3 + $Gly^{\bullet+}$) followed by H-atom abstraction by the newly formed $Gly^{\bullet+}$ from NH_3 (i.e. $Gly^{\bullet+}$ + NH_3 → $[Gly]H^+ + {}^\bullet NH_2$) yields $\mathbf{1b}^+$ in an overall exothermic reaction (by 25 kJ mol^{-1} based on $\Delta H_f°$ values from Scheme 1 and ref 45). The same final products may arise directly, via the proton transfer reaction Gly + $NH_3^{\bullet+}$ → $\mathbf{1b}^+ + {}^\bullet NH_2$.

(83) It is interesting to notice that parallel observations have been reported for the deprotonation of acetic acid by HO^-, which yields both CH_3COO^- and $^-CH_2COOH$ (82 kJ mol^{-1} less stable): Grabowski, J. J.; Cheng, X. *J. Am. Chem. Soc.* **1989**, *111*, 3106–3108.